Cd(9) and Cd(10) are also shown in Fig. 2. Centered around $\frac{1}{4}\frac{1}{4}\frac{3}{4}$ [Na(5)] are 12 Cd(8) forming a regular Friauf polyhedron (blue), and bridging over the surface are Cd(10) (yellow balls) completing a hexagon (transparent). The corners of the hexagons (yellow balls) form a small cubic arrangement of atoms. The central position of this cube is split in two - this is Cd(9) (red balls) with 50% occupancy. In other words, the blue Friauf polyhedron is intergrown with a b.c.c. structure to form an interpenetrating network in the structure. The Cd(8) and Cd(9) atoms form a building block denoted (3, 0) in our matrix notation, as shown in our parallel paper (Yang & Andersson, 1987).

The rest of the sodium atoms, as well as some cadmium atoms, are distributed over positions given in Table 1, with disorder; this is in the channel space obvious in Fig. 1. The structure is zeolitic in its character, which is reflected in its properties; crystals react with air or moisture, and gradually decompose.

We are grateful for valuable discussions with Docent C. Svensson. We also thank L. Thell for assistance with the calculations. QBY thanks the Royal Swedish Academy of Engineering for financial support. This research program is supported by the Swedish Research Council, which is gratefully acknowledged.

References

ANDERSSON, S., HYDE, S. T. & VON SCHNERING, H. G. (1984). *Z. Kristallogr.* **168**, 1-17.
HYDE, S. T. & ANDERSSON, S. (1984). *Z. Kristallogr.* **168**, 221-254.
HYDE, S. T. & ANDERSSON, S. (1986). *Z. Kristallogr.* In the press.
SAMSON, S. (1962). *Nature (London)*, **195**, 259-263.
SAMSON, S. (1965). *Acta Cryst.* **19**, 401-412.
YANG, Q. B. & ANDERSSON, S. (1987). *Acta Cryst.* **B43**, 1-14.

Acta Cryst. (1987). B43, 16-23

Thermal Vibration in CsSCN Below the Structural Phase Transition at 470 K*

BY B. K. MOSS AND S. L. MAIR

CSIRO Division of Chemical Physics, Clayton, Victoria 3168, *Australia*

G. J. MCINTYRE

Institut Laue-Langevin, 156*X*, *Centre de Tri*, 38042 *Grenoble, France*

AND R. K. MCMULLAN

Chemistry Department, Brookhaven National Laboratory, Upton, NY 11973, *USA*

(*Received* 27 *December* 1985; *accepted* 24 *June* 1986)

Abstract

Caesium thiocyanate undergoes a phase transition at $T_c \simeq 470$ K from an orthorhombic (*Pnma*) form to a cubic modification. Single-crystal neutron diffraction data have been obtained for CsSCN within the range 300 to 441 K and, together with reported data at 453 K, are analysed to study thermal motion in the crystal preceding the onset of the phase transition. For the SCN^- ions, the data are consistent with large rigid-body translations and librations, with only small contributions from internal modes. From 440 K to T_c, the SCN^- ions exhibit enhanced amplitudes of translational and librational motion; the Cs^+ ions exhibit a concomitant anomalous increase in vibrational amplitudes. This behaviour is highly anharmonic and is indicative of the onset of the phase transition at 470 K. The mechanism suggested for the phase transition involves a sudden rearrangement of all the ions at T_c. This is in contrast with KSCN, in which the phase transition arises purely by rotational disordering of the SCN^- ions.

Introduction

The thermal vibrational behaviour of solids in the vicinity of structural phase transitions may contain information on the nature of the phase transition. Presently there is a lack of both theoretical and experimental evidence on the temperature dependence of the thermal parameters obtained by Bragg diffraction from phase-transforming materials. Accurate experimental results are particularly scarce for the extended temperature region below phase transitions ($T < T_c$). See, however, the results of Lander, Brown & Faber (1982) on Cu_3Au. Temperature-dependent data above

* This paper should be regarded as forming part of the Ewald Memorial Issue of *Acta Cryst.* Section A published in November 1986.

0108-7681/87/010016-08$01.50

T_c have been obtained for several materials with soft-mode phase transitions, for example $CsPbCl_3$ (Sakata, Harada, Cooper & Rouse, 1980; Mair, 1982) and K_2SnCl_6 (Mair, 1984). A neutron powder diffraction study of $RbCaF_3$ by Bulou, Ridou, Rousseau, Nouet & Hewat (1980) provides data on both the low- and high-temperature sides of the soft-mode phase transition. In the immediate vicinity of T_c, work has been carried out on KH_2PO_4 and KD_2PO_4 by Nelmes, Kuhs, Howard, Tibballs & Ryan (1985) and on Cu_3Au by Lander & Brown (1985). See also the study of ferrocene (Seiler & Dunitz, 1979).

As part of a project to study structural phase transitions, with the eventual aim of attaining a deeper understanding of the information inherent in thermal vibrational parameters, we present neutron diffraction results for the compound CsSCN at temperatures below the phase transition at 470 K.

Caesium thiocyanate crystallizes as an orthorhombic layer structure of space group *Pnma* at room temperature and transforms to a cubic phase (a_0 = 4·83 Å) with the thiocyanate ion disordered at $T_c \simeq$ 470 K (Manolatos, Tillinger & Post, 1973). The transition was characterized as first order, on the basis of a discontinuous volume change and differential scanning calorimetry results. CsSCN may be compared with KSCN, which also has an orthorhombic layer structure (space group *Pbcm*) at room temperature, but which transforms at 473 K to a tetragonal structure (*I*4/*mcm*), the essential structural change being a rotational disordering of the SCN^- ions (Yamada & Watanabé, 1963). Yamada & Watanabé also observed a large expansion of the lattice, especially perpendicular to the layers, associated with the transition. Phase transitions isomorphous with that of KSCN probably also occur for the rubidium, ammonium and thallium thiocyanates (Klement, 1976). For a phase transformation of the KSCN type, librational modes for the SCN^- ion are expected to become dominant as T_c is approached. However, neutron inelastic scattering measurements of the temperature dependence of selected points on the CsSCN dispersion surface (Irving, Elcombe & Smith, 1984, 1985) have revealed no sign of any 'soft' phonon modes, librational or otherwise. On the other hand, single-crystal neutron diffraction results at 453 K (Irving, Elcombe & Smith, 1985) show large increases in the mean-square displacements of both the Cs^+ and SCN^- ions when compared with the room-temperature X-ray values of Manolatos, Tillinger & Post (1973). This suggests that the phase transformation is not solely related to the SCN^- ion disorder and that the phase transitions of CsSCN and KSCN occur by different mechanisms. Further evidence for this difference is discussed by Klement (1976).

Before the present work, Bragg diffraction data on CsSCN were available only at two temperatures, and the effect of thermal diffuse scattering (TDS) on vibrational parameters had not been accounted for at either temperature. It was therefore difficult to make any clear assessment of the thermal vibrational behaviour of CsSCN, and we were consequently motivated to carry out the following program:

(1) Measurements of single-crystal neutron diffraction data on CsSCN at temperatures from 300 to 441 K.

(2) Correction of the 453 K neutron diffraction data of Irving, Elcombe & Smith (1985) for TDS, with the cooperation of those authors.

(3) Analyses of these data for thermal motion in CsSCN between 300 and 453 K, including the consideration of rigid-body motion in the presence of internal vibrational modes.

Experiment

A cuboid of volume 26 mm^3 and maximum edge length 3·7 mm was shaped from a larger solution-grown crystal. Single-crystal neutron diffraction data were collected at 298, 373 and 428 K on the D9 diffractometer at the Institut Laue–Langevin (ILL) High Flux Reactor. The crystal was heated by immersion in a temperature-controlled dry air stream. The sample temperature was calibrated by reference to melting points of several crystals, each mounted at the sample position. The melting point of caesium thiocyanate itself was measured as 485 (1) K. This is 6 K higher than the value obtained by Manolatos, Tillinger & Post (1973). Temperature gradients across the sample were estimated by probing each face with a thermocouple. The maximum gradient was along the gas stream, being 6 K at 373 K and 12 K at 428 K. The stability of the experimental conditions was monitored by measuring three reference reflections (220, 222 and 020) after every 40 reflections. Fluctuations of some 1·5% about the mean intensities were recorded for the duration of the data collection at each temperature.

Of the three data sets collected at ILL, only that at 373 K was extensive enough (see Table 1) to provide highly accurate thermal parameters. A more complete but lower-resolution data set was subsequently measured at 441 K on the same crystal at the High Flux Beam Reactor, Brookhaven National Laboratory (BNL). The sample was heated in a vacuum furnace by conduction along a supporting aluminium pin affixed to a resistance-heated copper block. Temperatures within 1 K of preset values were maintained by thermocouple control elements embedded in the copper block near the sample support pin. Calibrations with test samples indicated temperatures 3 K less than the preset values. Background intensity scans over the entire 2θ range showed no significant contributions from powder diffraction lines arising from the aluminium pin or vacuum shroud. Experimental procedures for optimizing the crystal position in the beam, determining

Table 1. *Refined lattice parameters and experimental conditions*

Temperature (K)	298 (1)	373 (3)	428 (6)	441 (2)	453 (5)*
Monochromator	Cu(200)	Cu(200)	Cu(200)	Be(002)	Cu(220)
Wavelength (Å)	0·7025 (2)†	0·7025 (2)†	0·7025 (2)†	1·0504 (2)‡	1·238
Lattice parameters (Å) a_0	7·988 (3)	8·008 (3)	8·017 (3)	8·054 (2)	8·093 (7)
b_0	6·309 (2)	6·342 (3)	6·375 (3)	6·407 (2)	6·432 (5)
c_0	8·378 (3)	8·394 (4)	8·419 (4)	8·451 (2)	8·480 (7)
$(\sin\theta/\lambda)_{max}$ (Å^{-1})	0·815	0·958	0·807	0·779	0·552
Number of observed reflections	355	1657	242	2008	612
Number of independent sectors sampled	1	3	1	3	2
Number of independent reflections	268	797	221	732	341
Number of low-angle reflections omitted from final refinement because of extinction	9	4	4	4	0
$wR(F^2)$ for equivalent reflections	—	0·026	—	0·031	0·032
$wR(F^2)=[\sum w_i(F_i^2-F_{mean}^2)^2/\sum w_i(F_i^2)^2]^{1/2}$					
Absorption correction	Gaussian integration§	Gaussian integration§	Gaussian integration§	Analytical¶	Gaussian integration§

* Data of Irving, Elcombe & Smith (1985).
† Iridium foil in incident beam was used to absorb half-wavelength component of radiation.
‡ Determined by a least-squares fit of $\sin^2\theta$ values for a standard KBr crystal [$a_0=6·6000$ (13) Å at 298 K].
§ Coppens, Leiserowitz & Rabinovich (1965).
¶ Alcock (1970); de Meulenaer & Tompa (1965).

the orientation matrix (and lattice parameters), and fixing the intensity scan parameters followed those used in an earlier high-temperature study (Moss, McMullan & Koetzle, 1980). During data collection, the intensities of two reflections, 425 and 227, were monitored at approximately three-hour intervals: these varied less than 1·5% from the mean with no long-term trend apparent.

At all temperatures, the data were measured by $\theta/2\theta$ step scans with scan ranges determined from the dispersion observed at the wavelength and temperature of the study. Additional details of the experimental conditions are supplied in Table 1.

Data reduction

Observed squared structure factors were derived by correcting the integrated intensities for the effects of background, absorption, thermal diffuse scattering (TDS) and the Lorentz factor. For the ILL data the background was estimated using the method of Lehmann & Larsen (1974). For the BNL data the integrated intensity of 10% of the scan at either end of the range was used to estimate the background. Absorption corrections were small ($\mu=0·128$ cm^{-1} at $\lambda=1·05041$ Å and 0·161 cm^{-1} at $\lambda=0·7027$ Å) but were applied in order to evaluate the absorption-weighted path lengths required for refinement of the secondary extinction parameter.

The elastic constant values at 298 K required for TDS corrections of the room-temperature data were those reported by Irving, Prawer, Smith & Finlayson (1983). The temperature dependence of the terms on the diagonal of the elastic constant matrix were obtained by comparing the slopes of the phonon dispersion curves near $q=0$ at 293 and 453 K (Irving, Elcombe & Smith, 1984, 1985). The average softening of 7·7% was assumed to apply to the off-diagonal terms and linear interpolation was used to determine elastic constant values at intermediate temperatures. The ILL data were corrected for first- and second-order TDS using the program of Stevens (1974) modified for neutrons and for circular diffracted-beam apertures. All phonons were included in the calculation; the omission of faster-than-sound phonons has an effect of less than 0·1%. For the 441 K data and the data of Irving *et al.* at 453 K, the first-order TDS corrections α_1 were calculated with the program of Merisalo & Kurittu (1978) and the second-order TDS calculated empirically from the relation $\alpha_2=0·74\alpha_1^2$ deduced from the other data sets. Caesium thiocyanate is a fairly soft anisotropic material as evidenced by the thermal diffuse scattering; α values greater than 0·40 are typical for the 441 K data at $\sin\theta/\lambda$ greater than 0·7 Å^{-1}, and show a spread of about 35% at a given scattering angle. The highest correction was $\alpha_1+\alpha_2=1·6$ for the 0,10,0 reflection at 428 K.

In Table 1 are listed for each temperature the number of measurements, the number of independent reflections after averaging symmetry-related measurements and the corresponding internal agreement index. The standard deviations, σ, were determined according to Blessing (1986), whereby the experimental error estimate is modified by a function determined from the ratio of the standard deviation amongst symmetry-related reflections to the standard deviation from counting statistics. The revised σ's are larger than those determined solely from counting statistics. Table 1 contains the refined lattice parameters.

Refinement

An isotropic type 1 extinction model with a Lorentzian distribution was found to be most appropriate

for all five data sets (Becker & Coppens, 1974, 1975) in the least-squares refinements, which were based on observed squared structure factors. The extinction decreased appreciably on heating for the ILL experiments, while the 441 K data collected nine months later had extinction intermediate in size between that of the 373 and 428 K data. The extinction correction was large and judged to be inadequate for several of the low-angle reflections and so these were omitted from the final refinements (see Table 1). The nuclear coherent scattering lengths were taken from *International Tables for X-ray Crystallography* (1974). The caesium thiocyanate structure was essentially unchanged over the range of temperatures studied.

Three models to describe the thermal vibrations were considered: (i) unconstrained harmonic motion for all atoms; (ii) rigid-body motion of the thiocyanate ion, caesium unchanged; (iii) as for (ii) with the addition of the bond-bending internal mode contribution for the SCN^- ion, estimated from spectroscopic solid-phase data.

Rigid-body motion was treated with the TLX model of Pawley (1963), a constrained version of the TLS model (Schoemaker & Trueblood, 1968). The unconstrained refinements led to an almost linear geometry for the SCN^- ion and so exact linearity was assumed in the rigid-body refinements. As a result only two rigid-body librational modes were required. The corresponding mean-square angular displacements are denoted as L_{yy} (with librational axis along **b**) and L_{zz} (with axis mutually perpendicular to the SCN^- molecular axis and to **b**). The librational temperature factor used by us is given by equation (9) of Pawley & Willis (1970) (for the special case $\Omega_1 = r_2 = r_3 = 0$). This was derived assuming an effective one-particle potential describing *harmonic* librational motion. Although this temperature factor contains contributions to the first and third cumulants, only the former were found to be significant.

Correction for internal bond-bending modes

A linear geometry for the SCN^- molecule was also assumed in the treatment of bond-bending internal modes. This simplification allows a straightforward treatment of the internal modes of an isolated thiocyanate ion. The crystal field around the thiocyanate ion causes changes in the vibrational spectrum which have been considered by Taylor (1986). He determined that the frequencies of the bond-bending mode are thereby modified by about 1%.

If $C_{\infty v}$ symmetry is assumed, the normal modes of vibration of a linear isolated *XYZ*-type molecule are two bond-stretching modes (atoms moving parallel to molecular axis) and a doubly degenerate bending mode (atoms moving perpendicular to molecular axis). The magnitude of the refined rigid-body librations are only affected by the bond-bending mode, which can be estimated from spectroscopic data. (The bond-stretching modes affect the magnitude of the refined rigid-body translations in the direction of the molecular axis, but it is not possible to separate out the individual atomic contributions to the bond-stretching modes from the spectroscopic data alone.) Cyvin (1968) has described a method for determining the internal mode contribution to mean-square interatomic amplitudes, $\sum$, from the spectroscopic frequencies ν_j in the approximation of small harmonic vibrations by solving the secular equation

$$\sum G^{-1} - E\Delta = 0 \qquad (1)$$

where E is the identity matrix. The Δ values are related to the normal-mode frequencies ν_j by

$$\Delta_{jj} = (h/8\pi^2\nu_j c)\coth(h\nu_j c/2k_B T) \qquad (2)$$

and G^{-1}, the inverse kinetic energy matrix of Wilson (1939), depends only upon the atomic masses and atomic coordinates (Venkateswarlu, Mariam & Rajalakshmi, 1965).

The bond-bending contribution to $\sum$ is a diagonal term, $\sum_{22}$ (in the notation of Venkateswarlu *et al.*), and is of the form

$$\sum_{22} = \langle (Au_X^b + Bu_Y^b + Cu_Z^b)^2 \rangle \qquad (3)$$

where u_k^b is the bending-mode displacement perpendicular to the molecular axis for the kth atom (where $k = X$, Y or Z) and A, B, C are constants determined by the geometry of the molecule (Cyvin, 1968). By applying restrictions such that the origin is at the centre of mass of the molecule and the angular momentum is zero, (3) may be reduced to a function of any one of the three atomic displacements, of the form

$$\sum_{22} = A\langle (u_k^b)^2 \rangle \qquad (4)$$

where A is again a geometric constant. Numerical values for the required bond-bending mean-square displacements (m.s.d.'s), $\langle (u_k^b)^2 \rangle$, are then obtainable by substituting (4) and (2) in (1). Table 2 gives values of these m.s.d.'s for the SCN^- molecule, calculated using our refined values for the molecular bond lengths and the SCN^- solid-phase frequency data of Kinell & Strandberg (1959), quoted by Venkateswarlu *et al.* (1965).

Table 2. *Mean-square displacements perpendicular to the molecular axis due to the bond-bending internal modes*

	298 K	373 K	428 K	441 K	453 K
$\langle u^2_{\perp S} \rangle$ (Å^2)	0·000060	0·000068	0·000074	0·000077	0·000077
$\langle u^2_{\perp C} \rangle$ (Å^2)	0·00246	0·00277	0·00302	0·00315	0·00314
$\langle u^2_{\perp N} \rangle$ (Å^2)	0·000615	0·000693	0·000754	0·000722	0·000780

The total m.s.d.'s of the S, C and N are given by the sum of the internal and external mode

Table 3. *Positional, thermal and extinction parameters for refinements (i) – unconstrained, harmonic thermal vibrations*

Temperature (K)	298	373	428	441	453
Scale	11·45 (16)	11·68 (5)	11·60 (9)	235·0 (1·3)	3·28 (5)
Extinction ($\times 10^2$)	271 (17)	395 (21)	14 (4)	70 (2)	7·3 (4)
X_{Cs}	0·1782 (3)	0·1791 (1)	0·1793 (2)	0·1801 (1)	0·1801 (3)
Z_{Cs}	0·1060 (2)	0·10552 (9)	0·1048 (2)	0·10467 (8)	0·1047 (2)
U_{11Cs} (Å^2)	0·0411 (10)	0·0541 (4)	0·0631 (12)	0·0706 (4)	0·0719 (14)
U_{22Cs} (Å^2)	0·0418 (10)	0·0516 (4)	0·0604 (11)	0·0678 (4)	0·0724 (15)
U_{33Cs} (Å^2)	0·0404 (8)	0·0505 (4)	0·0618 (13)	0·0668 (3)	0·0675 (12)
U_{13Cs} (Å^2)	−0·0023 (9)	−0·0040 (3)	−0·0049 (9)	−0·0061 (3)	−0·0062 (10)
X_S	0·0197 (5)	0·0212 (2)	0·0232 (5)	0·0238 (2)	0·0253 (5)
Z_S	0·6893 (4)	0·6877 (2)	0·6873 (6)	0·6871 (2)	0·6863 (5)
U_{11S} (Å^2)	0·0380 (14)	0·0546 (8)	0·0664 (22)	0·0715 (8)	0·0741 (28)
U_{22S} (Å^2)	0·0616 (19)	0·0757 (11)	0·0931 (26)	0·0970 (12)	0·1072 (41)
U_{33S} (Å^2)	0·0433 (18)	0·0538 (7)	0·0635 (36)	0·0707 (8)	0·0787 (25)
U_{13S} (Å^2)	0·0022 (15)	0·0032 (7)	0·0017 (16)	0·0034 (6)	0·0028 (22)
X_C	0·1723 (2)	0·17300 (7)	0·1737 (2)	0·17425 (7)	0·1741 (2)
Z_C	0·5592 (1)	0·55898 (6)	0·5586 (2)	0·55882 (6)	0·5583 (2)
U_{11C} (Å^2)	0·0378 (8)	0·0484 (3)	0·0593 (9)	0·0641 (3)	0·0671 (11)
U_{22C} (Å^2)	0·0352 (8)	0·0452 (3)	0·0537 (9)	0·0600 (3)	0·0653 (12)
U_{33C} (Å^2)	0·0329 (5)	0·0420 (3)	0·0499 (8)	0·0565 (3)	0·0609 (10)
U_{13C} (Å^2)	−0·0032 (6)	−0·0048 (3)	−0·0049 (7)	−0·0063 (2)	−0·0066 (9)
X_N	0·2837 (2)	0·28365 (6)	0·2836 (2)	0·28384 (6)	0·2837 (2)
Z_N	0·4692 (1)	0·46913 (5)	0·4692 (2)	0·46893 (6)	0·4687 (2)
U_{11N} (Å^2)	0·0467 (7)	0·0598 (3)	0·0710 (7)	0·0797 (4)	0·0846 (11)
U_{22N} (Å^2)	0·0569 (7)	0·0697 (3)	0·0842 (8)	0·0928 (4)	0·0983 (12)
U_{33N} (Å^2)	0·0433 (5)	0·0552 (3)	0·0637 (8)	0·0725 (3)	0·0782 (10)
U_{13N} (Å^2)	0·0058 (5)	0·0066 (2)	0·0073 (6)	0·0084 (2)	0·0109 (8)

contributions. The internal mode contribution is fixed in the least-squares program and the external mode contribution is refined.

Results

The refined lattice parameters (Table 1) show that, from room temperature up to 428 K, lattice expansion is greatest in the **b** direction, perpendicular to the layers. Thereafter, the expansion increases markedly in all directions, an effect clearly associated with the approaching phase transition (see Fig. 1).

The refined parameters for model (i) are given in Table 3 and for models (ii) and (iii) in Table 4. For the data sets below 440 K the unconstrained refinements (i) give slightly better agreement factors (goodness of fits and *wR*'s) than the constrained refinements (Table 4). At the two highest temperatures, the constrained refinements (ii) (with four fewer parameters) give as good or better agreement factors, indicating that the SCN^- molecular vibrations are primarily rigid-body translations and librations. This conclusion was also supported by comparisons of the atomic m.s.d.'s in the SCN^- ion from model (i) projected along the bond direction. These generally agreed to within 0·001 Å^2, fulfilling the 'rigid-bond' postulate (Harel & Hirshfeld, 1975; Hirshfeld, 1976). The $\langle u_k^2 \rangle$ of the unconstrained (i) and rigid-body (ii) refinements were also in reasonable agreement; for all temperatures 58% agreed within 1σ and only 12% differed by more than 3σ. The $\langle u_k^2 \rangle$ for model (ii) are given in Table 5. Significantly longer bond lengths were obtained in case (ii), showing the importance of including the antisymmetric terms of the probability density function into the thermal motion description. The centre of libration of the SCN^- molecule refined to a position (X_L, $\frac{1}{4}$, Z_L) near the C atom and just off the molecular axis. This is illustrated for the 441 K data from refinement (ii) in Fig. 2, which also shows the structure of the layers. The results for the rigid-body refinements with

Table 4. *Refined positional, thermal and extinction parameters*

Temperature (K)		298	373	428	441	453
Scale		11·44 (15)	11·71 (5)	11·63 (9)	235·8 (1·3)	3·28 (4)
Extinction ($\times 10^2$)		267 (17)	41·2 (2·1)	15·8 (3·6)	70·2 (2·0)	7·4 (4)
X_{Cs}		0·1781 (3)	0·1791 (1)	0·1795 (2)	0·1800 (1)	0·1801 (3)
Z_{Cs}		0·1060 (2)	0·10554 (9)	0·1047 (2)	0·10475 (8)	0·1048(2)
U_{11Cs} (Å^2)		0·0420 (10)	0·0542 (4)	0·0637 (11)	0·0713 (4)	0·0722 (14)
U_{22Cs} (Å^2)		0·0421 (10)	0·0519 (4)	0·0608 (11)	0·0679 (4)	0·0728 (15)
U_{33Cs} (Å^2)		0·0405 (7)	0·0506 (4)	0·0623 (13)	0·0667 (3)	0·0676 (12)
U_{13Cs} (Å^2)		−0·0024 (9)	−0·0041 (3)	−0·0054 (9)	−0·0062 (3)	−0·0063 (10)
X_S		0·0187 (5)	0·0197 (2)	0·0217 (5)	0·0221 (2)	0·0231 (5)
Z_S		0·6899 (5)	0·6888 (2)	0·6884 (6)	0·6883 (2)	0·6878 (5)
X_C		0·1724 (2)	0·17323 (7)	0·1739 (2)	0·17458 (7)	0·1743 (2)
Z_C		0·5588 (2)	0·55862 (7)	0·5582 (2)	0·55823 (6)	0·5578 (2)
X_N		0·2849 (2)	0·28511 (6)	0·2854 (2)	0·28566 (6)	0·2857 (2)
Z_N		0·4681 (2)	0·46784 (6)	0·4676 (2)	0·46726 (6)	0·4669 (2)
T_{11} (Å^2)	(ii)	0·0360 (7)	0·0480 (3)	0·0580 (8)	0·0633 (3)	0·0658 (10)
	(iii)	0·0349 (6)	0·0463 (3)	0·0566 (8)	0·0619 (3)	0·0645 (10)
T_{22} (Å^2)	(ii)	0·0340 (9)	0·0442 (3)	0·0525 (10)	0·0584 (3)	0·0634 (12)
	(iii)	0·0316 (8)	0·0414 (3)	0·0495 (10)	0·0553 (3)	0·0603 (12)
T_{33} (Å^2)	(ii)	0·0332 (5)	0·0427 (3)	0·0501 (7)	0·0562 (2)	0·0607 (9)
	(iii)	0·0318 (5)	0·0411 (3)	0·0484 (7)	0·0545 (2)	0·0590 (9)
T_{13} (Å^2)	(ii)	−0·0040 (5)	−0·0053 (2)	−0·0059 (5)	−0·0074 (2)	−0·0074 (6)
	(iii)	−0·0053 (5)	−0·0067 (2)	−0·0074 (5)	−0·0090 (2)	−0·0089 (6)
L_{yy} (deg^2)	(ii)	32·0 (17)	38·4 (7)	44·5 (21)	49·3 (6)	56·0 (22)
	(iii)	35·3 (17)	42·3 (7)	48·8 (21)	53·7 (6)	60·3 (22)
L_{zz} (deg^2)	(ii)	37·6 (22)	42·1 (8)	55·0 (25)	54·1 (8)	55·4 (23)
	(iii)	40·8 (22)	46·0 (8)	59·2 (25)	58·6 (8)	59·8 (23)
X_L	(ii)	0·163 (4)	0·1571 (14)	0·163 (4)	0·1578 (11)	0·161 (3)
	(iii)	0·162 (4)	0·1575 (12)	0·163 (4)	0·1582 (09)	0·161 (3)
Z_L	(ii)	0·594 (4)	0·5865 (16)	0·585 (4)	0·5901 (12)	0·590 (3)
	(iii)	0·593 (4)	0·5852 (15)	0·583 (3)	0·5886 (11)	0·589 (3)
$wR(F^2)$	(i)	4·60	4·90	3·55	4·01	8·22
	(ii)	4·77	4·99	3·67	3·88	8·22
	(iii)	4·74	4·98	3·66	3·83	8·20
Goodness of fit, S	(i)	1·01	0·90	1·54	0·76	1·58
	(ii)	1·04	0·92	1·57	0·73	1·57
	(iii)	1·03	0·92	1·57	0·72	1·56

T_{11}, T_{22}, T_{33} and T_{13} are the components of the rigid-body translation matrix T of the thiocyanate ions. L_{yy} is the rigid-body libration in the *ac* plane; L_{zz} is the corresponding libration perpendicular to this plane. X_L and Z_L are fractional coordinates of the centre of libration.

$$S = \{[\sum_i w_i (F^2_{obs,i} - F^2_{calc,i})^2]/(m-n)\}^{1/2}$$

where m is the number of independent observations and n is the number of variables.

$$wR(F^2) = \{[\sum_i w_i (F^2_{obs,i} - F^2_{calc,i})^2]/[\sum_i (F^2_{obs,i})^2 w_i]\}^{1/2} \times 100.$$

Refined parameters in the first 14 rows are from refinement (ii) and agree with those of refinement (iii), generally to better than half a standard deviation.

Table 5. *Atomic mean-square displacements corresponding to model (ii) for sulfur, carbon and nitrogen*

Temperature (K)	298	373	428	441	453
U_{11S} (Å^2)	0·0422 (9)	0·0566 (4)	0·0684 (12)	0·0736 (4)	0·0775 (13)
U_{22S} (Å^2)	0·0564 (19)	0·0692 (7)	0·0869 (24)	0·0895 (7)	0·0958 (21)
U_{33S} (Å^2)	0·0461 (11)	0·0569 (5)	0·0675 (15)	0·0741 (4)	0·0818 (15)
U_{13S} (Å^2)	0·0049 (8)	0·0057 (3)	0·0076 (10)	0·0062 (3)	0·0083 (10)
U_{11C} (Å^2)	0·0369 (7)	0·0486 (3)	0·0586 (8)	0·0643 (3)	0·0671 (10)
U_{22C} (Å^2)	0·0351 (9)	0·0451 (3)	0·0535 (10)	0·0599 (3)	0·0649 (10)
U_{33C} (Å^2)	0·0333 (5)	0·0429 (3)	0·0565 (7)	0·0656 (2)	0·0609 (9)
U_{13C} (Å^2)	−0·0038 (5)	−0·0050 (2)	−0·0056 (5)	−0·0069 (2)	−0·0068 (6)
U_{11N} (Å^2)	0·0468 (7)	0·0596 (5)	0·0711 (14)	0·0794 (5)	0·0845 (15)
U_{22N} (Å^2)	0·0575 (9)	0·0704 (7)	0·0848 (24)	0·0936 (8)	0·0993 (22)
U_{33N} (Å^2)	0·0425 (5)	0·0550 (5)	0·0631 (13)	0·0721 (4)	0·0782 (14)
U_{13N} (Å^2)	0·0060 (5)	0·0066 (4)	0·0072 (10)	0·0086 (3)	0·0107 (11)

[case (iii)] and without [case (ii)] bond-bending internal mode contributions to the SCN^- molecular vibration are presented in Table 4. Although the SCN^- bond-bending modes are comparatively small their inclusion causes significant increments in both the in- and out-of-plane libration parameters (L_{yy} and L_{zz}, respectively) and reductions in the rigid-body translational parameters, with a slight overall improvement in the agreement. The higher frequency bond-stretching modes would be expected to have a considerably smaller effect on the rigid-body parameters [see equation (2)].

The m.s.d.'s for the Cs^+ and SCN^- ions and the mean-square angles of libration for the SCN^- ion are presented as functions of temperature in Figs. 3 and 4. Also shown are straight lines through the origin, intended as references for purely harmonic vibration. All components of the translational vibration of both ions are seen to increase anomalously as the phase transition is approached from below. This behaviour is also observed for the in-plane libration, the r.m.s. angle of libration reaching a value of 7·8°. A similar trend may be present for the out-of-plane libration, but L_{zz} is not sufficiently well determined for a definite conclusion. The anomalous rises in the temperature parameters are too large to be due to anharmonic perturbations, which add a T^2 term to the temperature dependence of the m.s.d., to first order [as, for

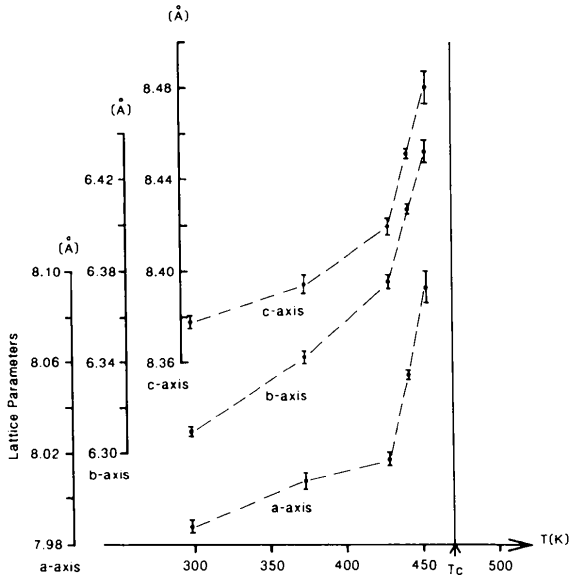

Fig. 1. The temperature dependence of the lattice parameters. The 453 K data are from Irving, Elcombe & Smith (1985).

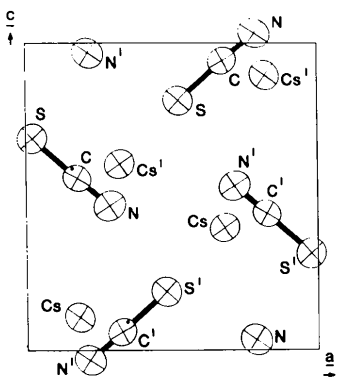

Fig. 2. The caesium thiocyanate structure in projection down the b axis. The primed atoms are at $y=\frac{3}{4}$; the remainder are at $y=\frac{1}{4}$. The refined centres of libration are indicated with small dots (for the 441 K data). Thermal ellipsoids are shown at the 50% probability level (Johnson, 1976).

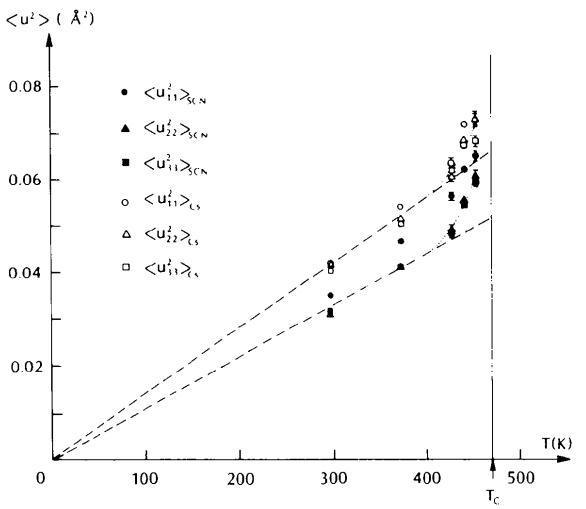

Fig. 3. The temperature dependence of the m.s.d.'s for the Cs^+ ion, and the rigid-body translations of the SCN^- ion, from refinements (iii), including the bond-bending internal modes. The dashed lines are included as a guide to the eye.

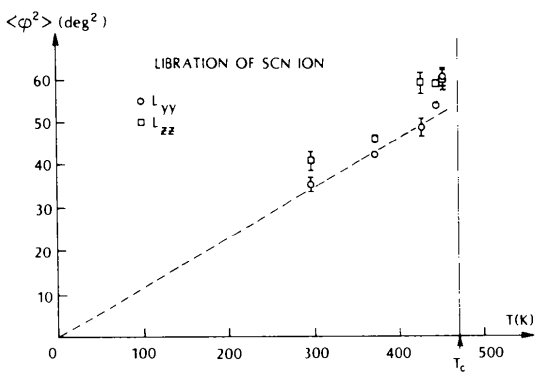

Fig. 4. Temperature dependence of the in- and out-of-plane libration parameters (L_{yy} and L_{zz} respectively) for the thiocyanate ion, from refinements (iii).

example, in SrF_2, Mair, Barnea, Cooper & Rouse (1974)], and we attribute the phenomenon to precursor effects associated with the phase transition at 470 K.

It is sometimes useful to consider the non-linear dependence of the m.s.d.'s upon temperature in terms of a softening of the quadratic term in an effective one-particle potential, $\varphi^k_{\alpha\alpha}$, where α denotes a Cartesian coordinate and k the atomic species. In the classical regime we have

$$\varphi^k_{\alpha\alpha} = 8\pi^2 k_B T / \langle u^2{}_{\alpha\alpha} \rangle_k. \quad (5)$$

The $\varphi^k_{\alpha\alpha}$ determined by substituting our experimental $\langle u^2_k \rangle$ in (5) are fairly isotropic and show softenings of 9·6% for the Cs ion and 13·4% for the rigid-body translational force constants of the SCN^- molecule, both taken over the temperature range 373 to 453 K. Similar results are obtained from the individual S, C and N m.s.d.'s of our type (i) refinements. For comparison, the maximum reduction in $\varphi^k_{\alpha\alpha}$ for the slightly anharmonic crystal, SrF_2, over a similar temperature range is 3·4% (for the F ion) whereas for a truly harmonic crystal it is zero.

Discussion

To the best of our knowledge, the present work represents the first reported temperature-dependent study of librational mean-square displacements in which pre-transitional effects are apparent. Although the detailed nature of the phase transition is still not clear, we are able to make some suggestions as to its probable nature.

The anomalous increase in practically all of the thermal vibrational parameters, rather than in just those of one type of ion in some specific direction(s) [*cf.*, for example, $RbCaF_3$ (Bulou *et al.*, 1980) or K_2SnCl_6 (Mair, 1984)], indicates that the phase transition probably involves shifts of all the atoms.

Trends in the positional parameters as a function of temperature are apparent, but do not appear to obey the mechanism of transformation to a primitive cubic form proposed by Manolatos *et al.* (1973). The fact that the volume of the unit cell at 453 K is about four times the volume of the unit cell in the cubic phase is suggestive that some simple structural relationship exists between the two phases. However, no pseudocubic lattice is present at this temperature and it appears that there must be a sudden rearrangement of the atoms very close to T_c.

In considering atomic rearrangements in the low-temperature phase, it should be noted that out-of-plane rotations of the SCN^- ion are inhibited by the close proximity of the Cs^+ ions in the adjacent layer. A disordering which involves relatively free out-of-plane rotations would therefore require the Cs^+ ions to move. This is in contrast with KSCN, where relatively free out-of-plane rotation of the SCN^- ion can be achieved without movement of the cations.

Although the selective examination of the phonon dispersion surface (principally of the acoustic modes) by Irving *et al.* (1984, 1985) did not reveal any soft phonon modes, our results are not inconsistent with their presence. The trend in the m.s.d.'s and in the mean-square angular displacements (L_{yy} and L_{zz}) with temperature is quite similar to that of certain components of the m.s.d. of the F^- ions in the tetragonal phase of $RbCaF_3$ (Bulou *et al.*, 1980), where soft modes are probably present (Boyer & Hardy, 1981). Molecular dynamics calculations (Mair, 1986) of the m.s.d. through a soft-mode phase transition are also qualitatively similar to the present experimental results for CsSCN.

A final point concerns the softening with temperature of the elastic constants compared with the one-particle quadratic force constants. The elastic constants are dependent only on the long-wavelength acoustic phonon modes of vibration, whereas the $\varphi^k_{\alpha\alpha}$ may also show significant effects from any modes which are low (soft) enough to contribute to the $1/\omega^2$ dependence of the m.s.d.'s. The temperature dependence of the diagonal terms in the elastic constant matrix (derived from the dispersion data of Irving *et al.*, 1984, 1985) are, unlike the $\varphi^k_{\alpha\alpha}$, fairly anisotropic and reduce by an average of 7·7% over the temperature range 298 to 453 K. Over the same temperature range, the $\varphi^k_{\alpha\alpha}$ derived from the translational m.s.d.'s reduce by 10·1% and 17·7% for the Cs^+ and SCN^- ions, respectively. The relatively larger decrease in the $\varphi^k_{\alpha\alpha}$ compared with the elastic constants is therefore suggestive of the presence of soft modes.

The authors wish to thank Mark Irving for the crystals of caesium thiocyanate and Margaret Elcombe for providing details of the data collection at 453 K. We are grateful to Dr Mogens Lehmann for facilitating the experiment at ILL and for providing one of the crystal melting-point standards. Research at Brookhaven National Laboratory was performed under contract DE-AC-02-CH00016 with the US Department of Energy, and supported by its Division of Basic Energy Sciences. BM gratefully acknowledges the support of a CSIRO postdoctoral fellowship.

References

ALCOCK, N. W. (1970). *Crystallographic Computing*, edited by F. R. AHMED, p. 271. Copenhagen: Munksgaard.

BECKER, P. J. & COPPENS, P. (1974). *Acta Cryst.* A**30**, 129-147, 148-153.

BECKER, P. J. & COPPENS, P. (1975). *Acta Cryst.* A**31**, 417-425.

BLESSING, R. H. (1986). *Crystallogr. Rev.* **1**. In the press.

BOYER, L. L. & HARDY, J. R. (1981). *Phys. Rev. B*, **24**, 2577-2591.

BULOU, A., RIDOU, C., ROUSSEAU, M., NOUET, J. & HEWAT, A. (1980). *J. Phys. (Paris)*, **41**, 87-96.

COPPENS, P., LEISEROWITZ, L. & RABINOVICH, D. (1965). *Acta Cryst.* **18**, 1035-1038.
CYVIN, S. J. (1968). *Molecular Vibrations and Mean-Square Amplitudes.* Oslo: Universitetsforlaget.
HAREL, M. & HIRSHFELD, F. L. (1975). *Acta Cryst.* B**31**, 162-172.
HIRSHFELD, F. L. (1976). *Acta Cryst.* A**32**, 239-244.
International Tables for X-ray Crystallography (1974). Vol. IV. Birmingham: Kynoch Press. (Present distributor D. Reidel, Dordrecht.)
IRVING, M. A., ELCOMBE, M. M. & SMITH, T. F. (1984). *Aust. J. Phys.* **37**, 287-303.
IRVING, M. A., ELCOMBE, M. M. & SMITH, T. F. (1985). *Aust. J. Phys.* **38**, 85-95.
IRVING, M. A., PRAWER, S., SMITH, T. F. & FINLAYSON, T. R. (1983). *Aust. J. Phys.* **36**, 85-92.
JOHNSON, C. K. (1976). *ORTEP*II. Report ORNL-5138. Oak Ridge National Laboratory, Tennessee.
KINELL, P. O. & STRANDBERG, B. (1959). *Acta Chem. Scand.* **13**, 1607-1622.
KLEMENT, W. J. (1976). *Bull. Chem. Soc. Jpn*, **49**, 2148-2153.
LANDER, S. H. & BROWN, P. J. (1985). *J. Phys. C*, **18**, 2017-2024.
LANDER, S. H., BROWN, P. J. & FABER, J. (1982). *J. Phys. C*, **15**, 6699-6708.
LEHMANN, M. S. & LARSEN, F. K. (1974). *Acta Cryst.* A**30**, 580-584.
MAIR, S. L. (1982). *Acta Cryst.* A**38**, 790-796.
MAIR, S. L. (1984). *Solid State Commun.* **52**, 335-337.
MAIR, S. L. (1986). *J. Phys. C.* In the press.
MAIR, S. L., BARNEA, Z., COOPER, M. J. & ROUSE, K. D. (1974). *Acta Cryst.* A**30**, 806-813.
MANOLATOS, S., TILLINGER, M. & POST, B. (1973). *J. Solid State Chem.* **7**, 31-35.
MERISALO, M. & KURITTU, J. (1978). *J. Appl. Cryst.* **11**, 179-183.
MEULENAER, J. DE & TOMPA, H. (1965). *Acta Cryst.* **19**, 1014-1018.
MOSS, B., MCMULLAN, R. K. & KOETZLE, T. F. (1980). *J. Chem. Phys.* **73**, 495-508.
NELMES, R. J., KUHS, W. F., HOWARD, C. J., TIBBALLS, J. E. & RYAN, T. W. (1985). *J. Phys. C*, **18**, L711-716.
PAWLEY, G. S. (1963). *Acta Cryst.* **16**, 1204-1208.
PAWLEY, G. S. & WILLIS, B. T. M. (1970). *Acta Cryst.* A**26**, 260-262.
SAKATA, M., HARADA, J., COOPER, M. J. & ROUSE, K. D. (1980). *Acta Cryst.* A**36**, 7-15.
SCHOEMAKER, V. & TRUEBLOOD, K. N. (1968). *Acta Cryst.* B**24**, 63-76.
SEILER, P. & DUNITZ, J. D. (1979). *Acta Cryst.* B**35**, 1068-1074, 2020-2032.
STEVENS, E. D. (1974). *Acta Cryst.* A**30**, 184-189.
TAYLOR, P. R. (1986). *J. Am. Chem. Soc.* Submitted.
VENKATESWARLU, K., MARIAM, S. & RAJALAKSHMI, K. (1965). *Acad. R. Sci. Lett. B.-Arts Belg. Cl. Sci. Bull.* **51**, 359-370.
WILSON, G. (1939). *J. Chem. Phys.* **2**, 1047-1052.
YAMADA, Y. & WATANABÉ, T. (1963). *Bull. Chem. Soc. Jpn*, **36**, 1032-1037.

Acta Cryst. (1987). B**43**, 23-28

Dependence of the Distortion of the Tetrahedra in Acid Phosphate Groups H_nPO_4 ($n = 1$–3) on Hydrogen-Bond Length

BY MIZUHIKO ICHIKAWA

Department of Physics, Faculty of Science, Hokkaido University, Sapporo 060, *Japan*

(*Received* 27 *January* 1986; *accepted* 8 *July* 1986)

Abstract

The distortions of the PO_4 tetrahedra of acid phosphate groups H_nPO_4 ($n = 1$-3) have been studied by examining the correlations of the P-O bond lengths, OPO angles, O–O lengths and Baur's distortion indices with the hydrogen-bond length O–H···O. All three distortion indices correlate with O–H···O, indicating that the PO_4 distortion becomes larger with an increase in O–H···O. The individual or average P–O lengths, OPO angles and O–O lengths also correlate with O–H···O. This is most pronounced for P–O, least for O–O. The mean values of P–O, OPO and O–O are reasonably constant in each H_nPO_4 type, most notably in the case of OPO. The dependence of the PO_4 distortion on O–H···O can be described approximately by a model in which the P atom shifts away from the centroid of the regular tetrahedral framework, while retaining $3m$ site symmetry for HPO_4-type structures and $mm2$ symmetry for H_2PO_4-type structures.

Introduction

The bond lengths and angles of structural moieties in crystals, for example, tetrahedral XO_4-type ions and carboxyl groups, are known to deviate from regularity depending on the number and kinds of neighboring cations. For PO_4 groups the deviation from a regular tetrahedral arrangement has been extensively investigated by Baur (1974) for various kinds of PO_4 groups in crystals. He examined the P–O distances, O–P–O angles, O–O distances, their distortion indices and the bond strengths, and clarified the basic characteristics of the distortion of PO_4 groups in crystals.

The strengths of hydrogen bonds around a moiety contribute to the environmental effect. It seems to be recognized as a general rule for crystals that, when H is attached to XO_4 groups, the bond lengths are intermediate between those for the ion without the proton and those for the same ion with a residue attached (Cruickshank, 1961). However, as the effects of hydrogen-bond length are not pronounced and are

0108-7681/87/010023-06$01.50